数理解析研究所講究録
第536巻 1984年 201-214

A Chaotic Attractor from a 2-segment Piecewise-linear Capacitor Circuit

S. Tanaka (田中 聡)
Department of Electrical Engineering,
Waseda University,
Tokyo 160, Japan

T. Matsumoto (松本 隆)
Department of Electrical Engineering,
Waseda University,
Tokyo 160, Japan

L. O. Chua
Department of Electrical Engineering
and Computer Sciences,
University of California, Berkeley,
California, 94720

A B S T R A C T

An extremely simple non-autonomous circuit is considered. This circuit is so simple that it is easy to understand the structure of the chaotic attractor.

1. INTRODUCTION

It is well known that a driven R-L-Diode circuit of Fig. 1 exhibits period doubling, chaotic behavior and periodic windows [1], [2], [3].

There have been explanations for the cause of such behavior [3], [4], [5], [6]. Those explanations, however, are rather complicated. In order to study the "cause" for the chaotic behavior, we have

simplified the model for the diode [7] and considered the circuit of Fig. 2(a) with the capacitor characteristic given by Fig. 2(b). The bifurcation diagram given in [7] resmbles, in a surprisingly close manner, the experimental observations [2], [3] and the computer simulations with much more complicated models [4], [5], [6]. This indicates that the nonlinearity of the capacitor is at least one cause for the chaotic behavior of driven R-L-Diode circuits. Our purpose here is to study the "structure" of a chaotic attractor observed with the driven R-L-C circuit.

Note that the dynamics of the circuit of Fig. 2 is described by

$$\frac{dq}{dt} = i \tag{1}$$

$$L\frac{di}{dt} = -Ri - v(q) + E\sin\omega t$$

where q is the capacitor charge, i is the current, L is the inductance, R is the resistance, v(q) is the q-v characteristic of the 2-segment piecewise-linear capacitor, E is the amplitude of the driving voltage source and $\omega/2\pi$ is the frequency.

Interesting chaotic attractors other than the one reported in [7] have been observed. Fig. 3 shows two of them. Our purpose here is to make a further simplification of (1) and study the structure of the attractor shown in Fig. 3(a).

2. THE STRUCTURE

Here we will replace the sinusoidal driving force of (1) with a square driving force. The dynamics, then, is given by

$$\frac{dq}{dt} = i$$

$$\frac{di}{dt} = -\frac{R}{L}i - \begin{cases} \frac{1}{LC_1}q & \text{if } q \geq 0 \\ \frac{1}{LC_2}q & \text{otherwise} \end{cases} + \begin{cases} +\frac{E}{L} & \text{if } nT < t \leq (n+\frac{1}{2})T \\ -\frac{E}{L} & \text{if } (n+\frac{1}{2})T < t \leq (n+1)T \end{cases} \tag{2}$$

$(E_o = 0)$

By appropriate rescaling, (2) is transformed into

$$\frac{dq}{dt} = i$$

$$\frac{di}{dt} = -ki - \begin{cases} \alpha q & \text{if } q \geqq 0 \\ \beta q & \text{otherwise} \end{cases} + \begin{cases} +1 & \text{if } nT < t \leqq (n+\frac{1}{2})T \\ -1 & \text{if } (n+\frac{1}{2})T < t \leqq (n+1)T \end{cases} \tag{3}$$

with $k = 0.7$, $\alpha = 0.1$, $\beta = 10.0$, and $\omega/2\pi = 0.22$, the attractor of Fig. 4 has been observed, which seems to be qualitatively the same as that of Fig. 3(a).

One of the greatest advantages of considering (3) instead of (1) is that the dynamics of (3) can be explained in terms of the following four linear autonomous flows on $\mathbb{R}^2$:

(i) $q \geqq 0$ and the driving force is +1

(ii) $q < 0$ and the driving force is +1

(iii) $q \geqq 0$ and the driving force is -1

(iv) $q < 0$ and the driving force is -1

Assumption :

(i) The cross section of the attractor at $t=nT$ is contained in the fourth quadrant.

(ii) The cross section of the attractor at $t=nT+\frac{T}{2}$ is contained in the first quadrant.

Let φ^t be the flow generated by (3) and let $\varphi_1{}^t$, $\varphi_2{}^t$, $\varphi_3{}^t$ and $\varphi_4{}^t$ be the linear flows coresponding to (i), (ii), (iii) and (iv), respectively (Fig. 5). In order to study the attractor, we consider the following two situations:

Case 1 The driving force in +1

Figure 6 shows the flows $\varphi_1{}^t$ and $\varphi_2{}^t$. Consider the curve ℓ which is the orbit of the system passing through the origin and pick a "thin" rectangle A as in the figure. We study how A is deformed while it is flowing along φ^t. To this end, pick an initial condition (q_o, i_o) (in A) on the right hand side of ℓ. The $\varphi_1{}^t(q_o, i_o)$ never hits the i-axis until $t = T/2$. On the other hand, if one picks an initial condition (q_o, i_o) on the left hand side of ℓ, then $\varphi_1{}^t(q_o, i_o)$ eventually hits the i-axis: $(q_1, i_1) \triangleq \varphi_1{}^{t_1}(q_o, i_o)$. After $t = t_1$, the dynamics obeys the flow $\varphi_2{}^t$. After a while $\varphi_2{}^t(q_1, i_1)$ again hits the i-axis: $(q_2, i_2) \triangleq \varphi_2{}^{t_2}(q_1, i_1)$, and then flows along with $\varphi_1{}^t$ after

$t = t_2 + t_1$. The key observation here is that $\alpha < \beta$ (α=0.1, β=10.0) implies that the velocity in the vertical direction for ${\varphi_2}^t$ is <u>larger</u> than that for ${\varphi_1}^t$. This, in turn, implies that the part of A which is on the left hand side is <u>stretched in the vertical direction</u> while flowing along with ${\varphi_2}^t$ and then compressed while flowing along with ${\varphi_1}^t$. The part of A which is on the right hand side of ℓ is always compressed in the vertical direction. As a result, one sees the <u>folded</u> objects B and C in Fig. 6.

<u>Case 2 The driving force is -1</u>

After $t = T/2$, the dynamics obeys ${\varphi_3}^t$ and ${\varphi_4}^t$ (Fig. 7). It follows from our assumption that $\varphi^t(C)$ never gets into the region of ${\varphi_4}^t$ for $nT + \frac{T}{2} < t \leq (n + 1)T$. This implies that the object C is slowly compressed in the vertical direction and returns to the original region where A is located.

If the above process is repeated many times, then the <u>stretching and folding</u> give rise to complicated behavior. One can also observe, numerically, how an appropriate region containing A comes back into itself after each period. The whole picture is given in Fig. 8. More Details will be reported elsewhere.

<u>ACKNOWLEDGEMENT</u>:

We would like to thank M. Ochiai, N. Kakiuchi, S. Ichiraku, M. Komuro, T. Saito, M. Kurokawa and K. Kobayashi for discussions.

Reference

1. P.S. Linsay, Phys. Rev. Lett. <u>47</u> 1349 (1981)
2. J. Testa, J. Perez and C. Jeffries, Phys. Rev., Lett, 48, 714 (1982)
3. S. D. Brorson, D. Dweney, and P.S. Linsay, Phys. Rev. A <u>28</u> <u>1201</u> (1983)

4. R.W. Rollins and E.R. Hunt, Phys. Rev. Lett, 49 1295 (1982)
5. A. Azzouz, M. Hasler and R. Duhr, IEEE Trans., CAS, 30 913 (1983)
6. A. Azzouz, R. Duhr and M. Hasler, IEEE Trans., CAS, to appear
7. T. Matsumoto, L.O. Chua, S. Tanaka, Phys. Rev. A, August, 1984

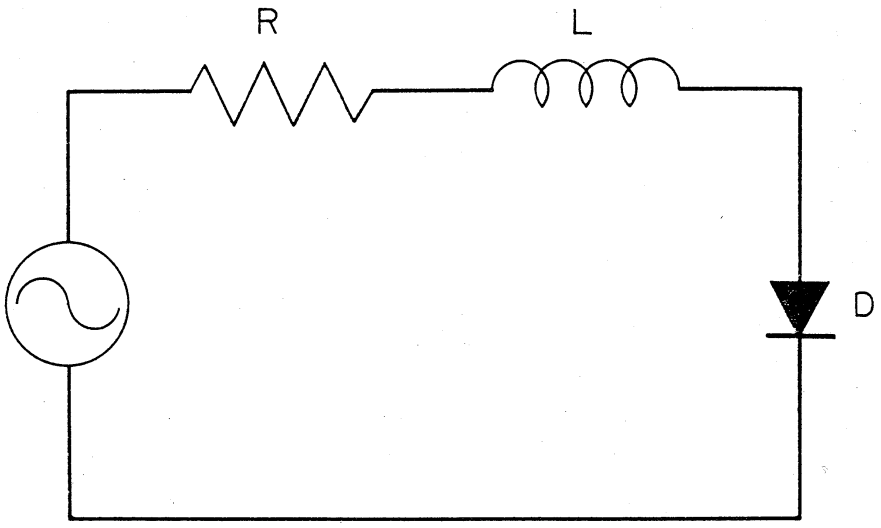

Fig. 1

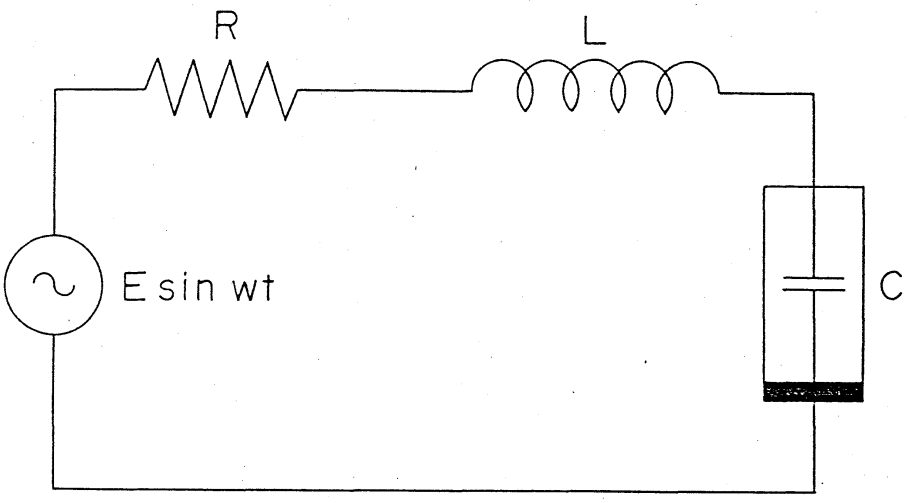

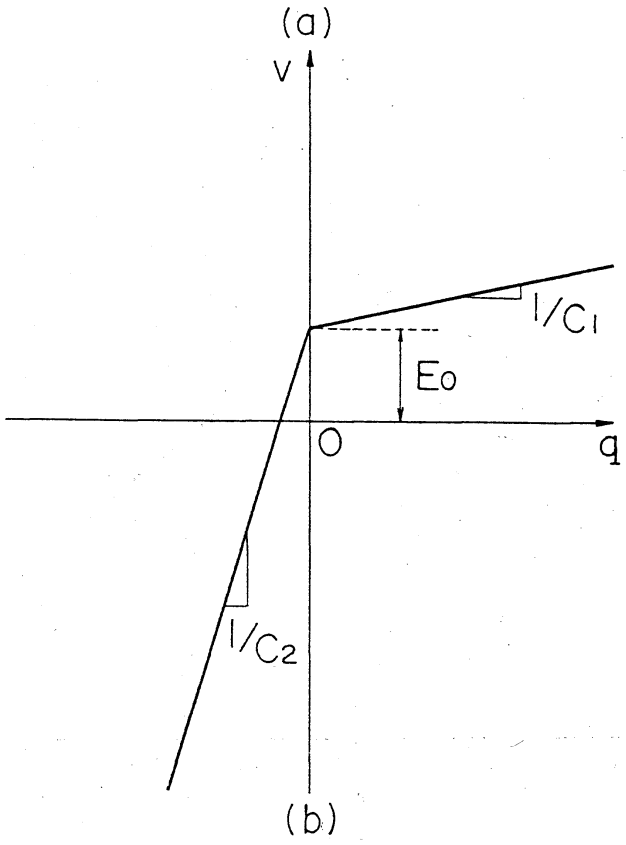

Fig 2

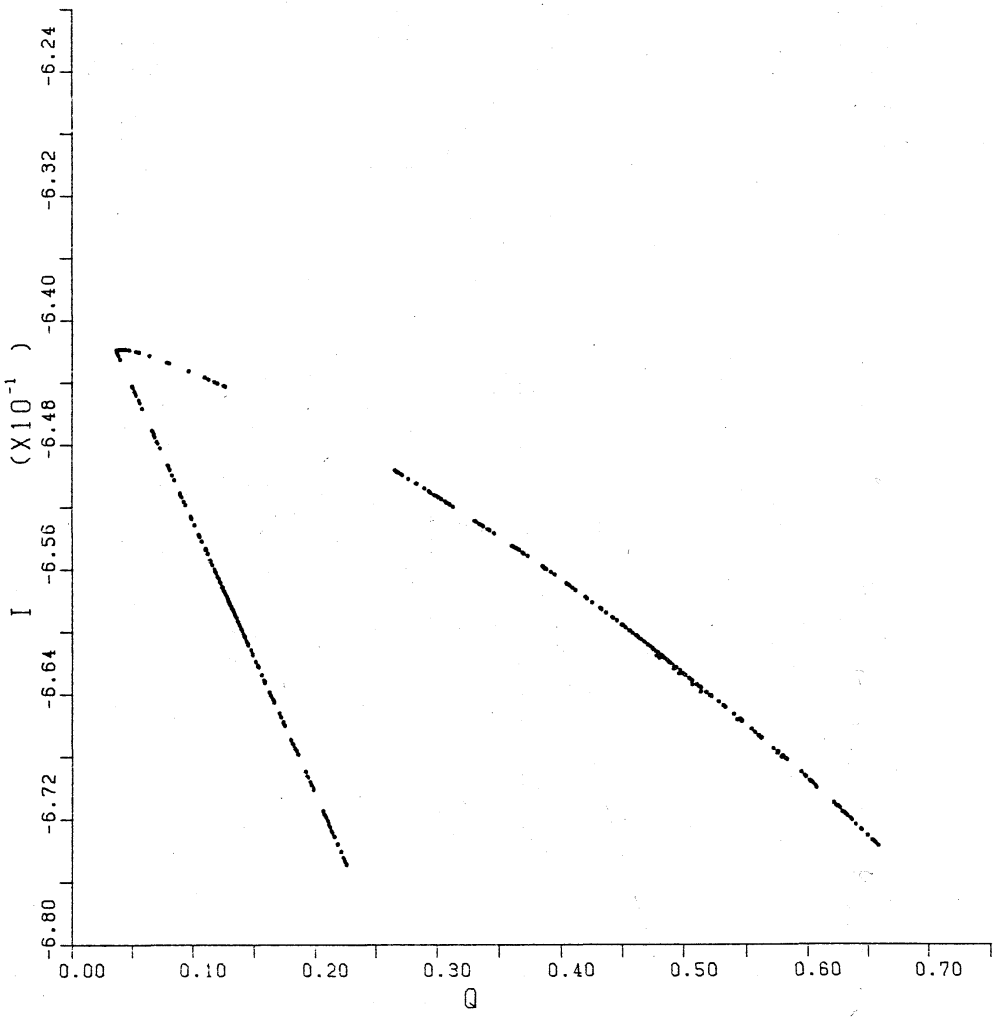
I (X10⁻¹)
-6.24
-6.32
-6.40
-6.48
-6.56
-6.64
-6.72
-6.80
0.00
0.10
0.20
0.30
0.40
0.50
0.60
0.70
Q

Fig 3 (a)

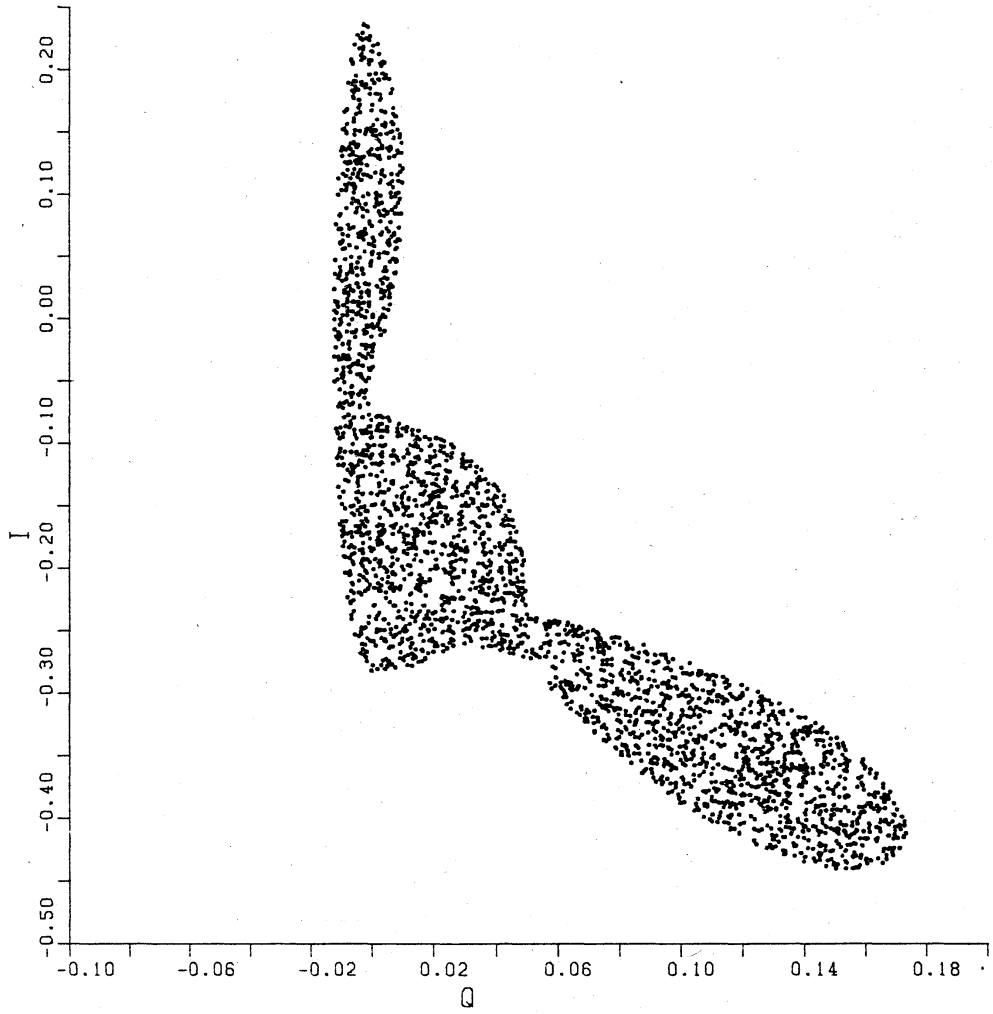
0.20
0.10
0.00
-0.10
-0.20
-0.30
-0.40
-0.50
I
-0.10
-0.06
-0.02
0.02
0.06
0.10
0.14
0.18
Q

Fig 3 (b)

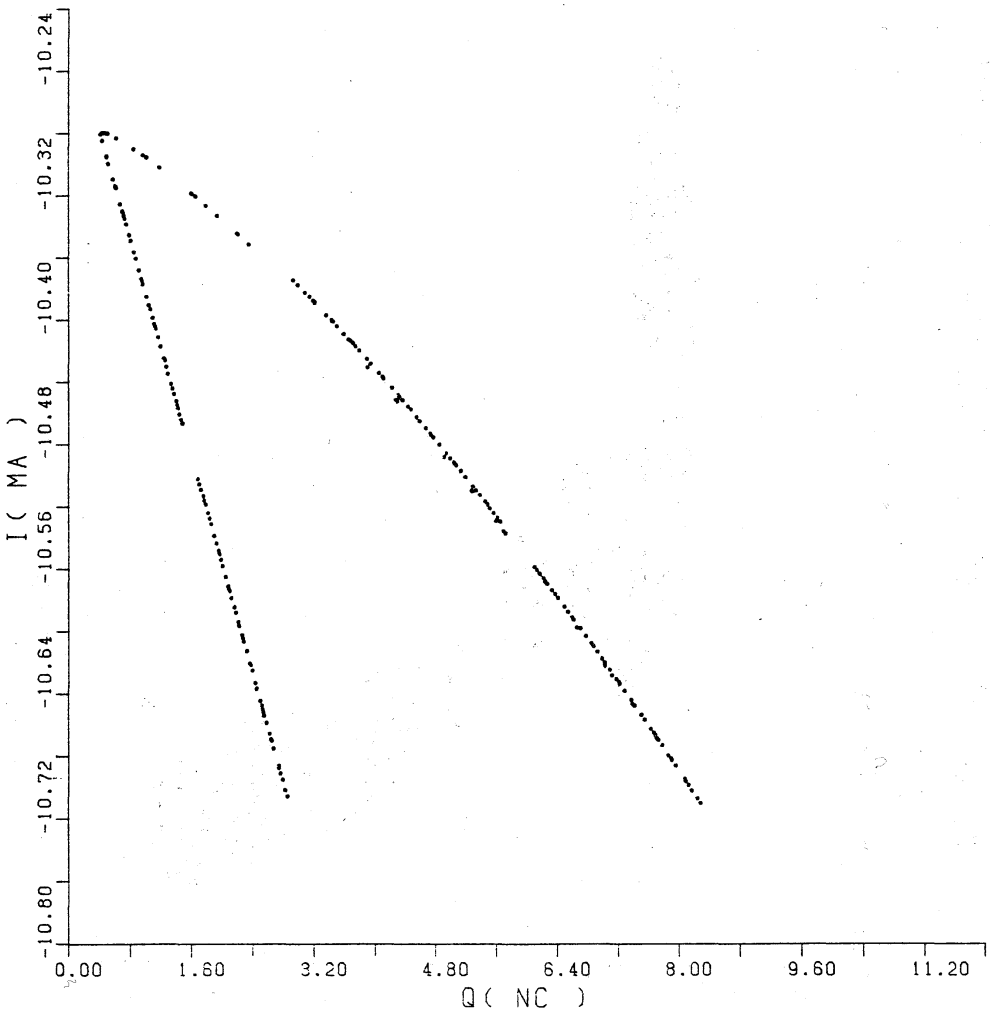
I(MA)
-10.24
-10.32
-10.40
-10.48
-10.56
-10.64
-10.72
-10.80
0.00
1.60
3.20
4.80
6.40
8.00
9.60
11.20
Q(NC)

Fig 4

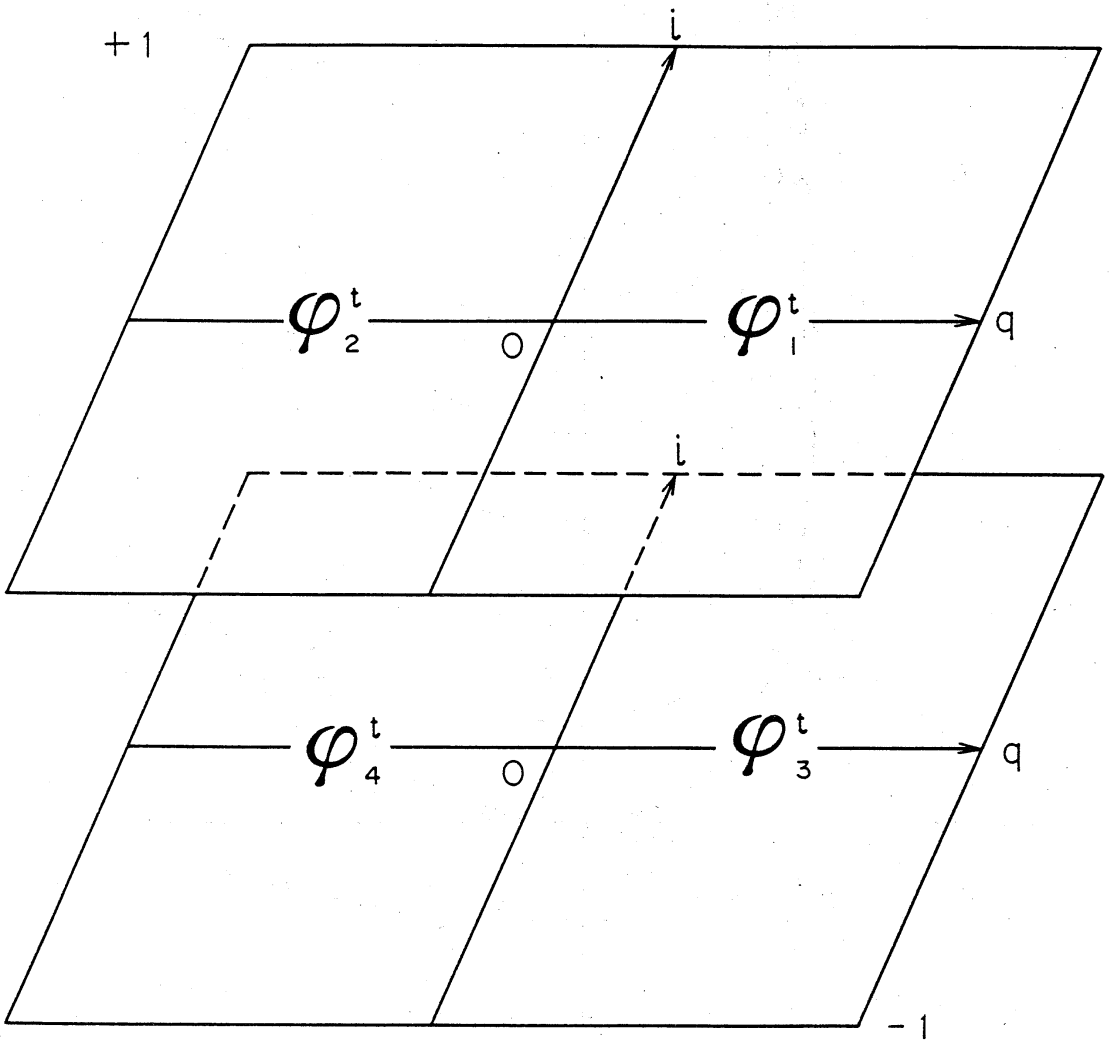

Fig. 5

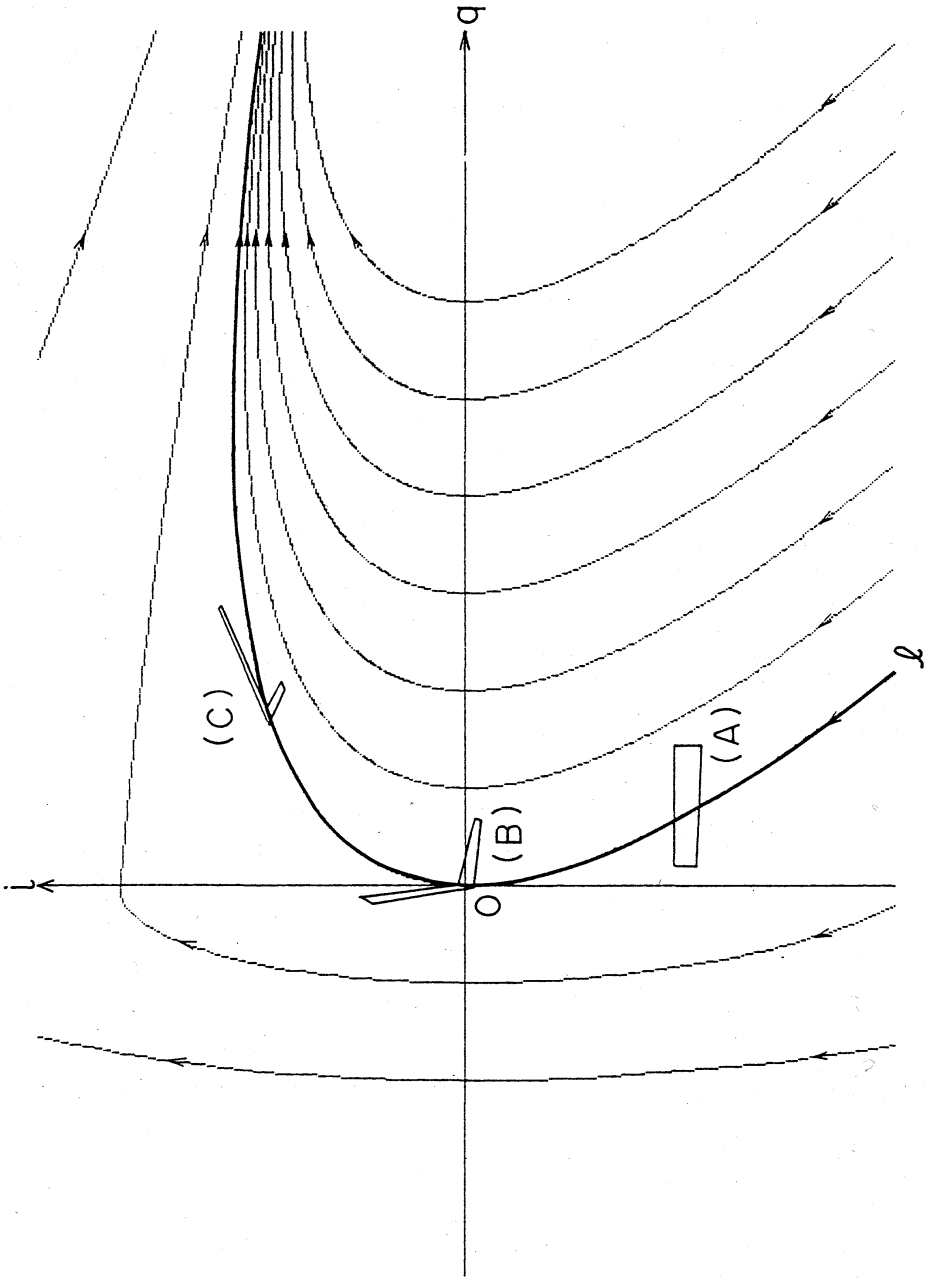

Fig. 6

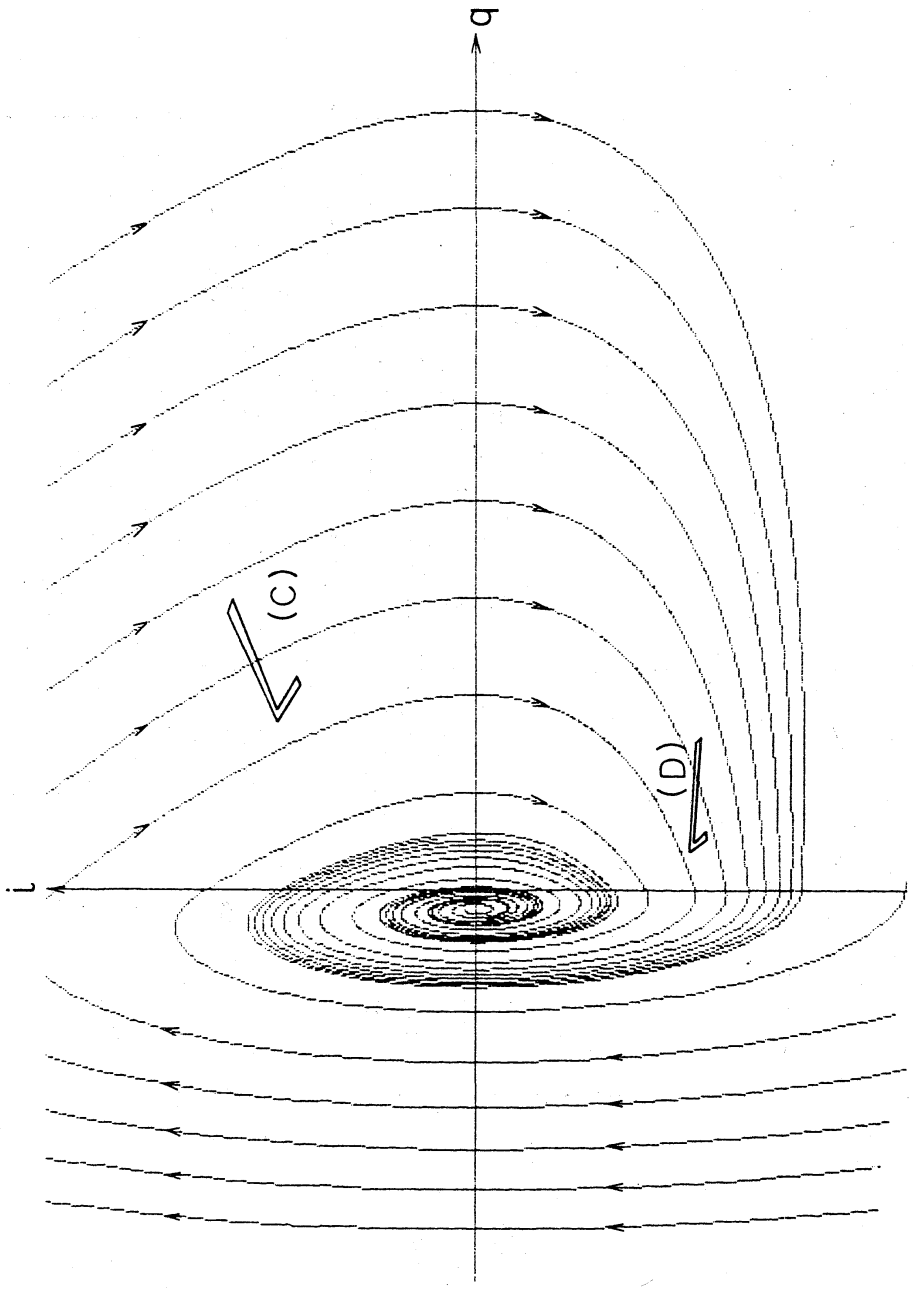

Fig. 7

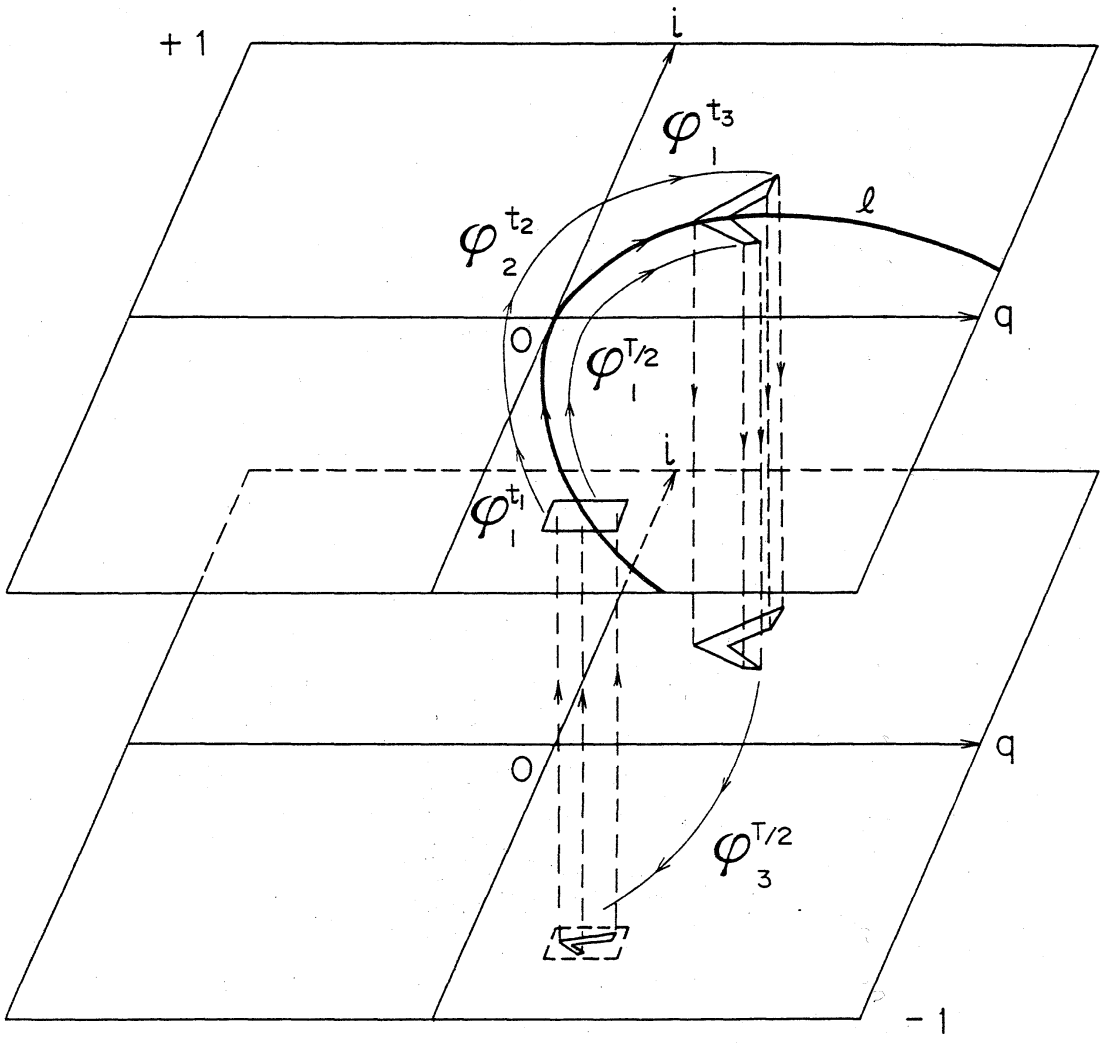
+1
i
$\varphi_1^{t_3}$
$\varphi_2^{t_2}$
ℓ
q
0
$\varphi_1^{T/2}$
i
$\varphi_1^{t_1}$
q
0
$\varphi_3^{T/2}$
-1

Fig. 8